materials

MDPI

Article

Solid State Phase Equilibria of an Al–Sn–Y Ternary System

Wenchao Yang [1,2,4], Moumiao Liu [2,4], Junli Feng [3], Jingwu Wu [3], Jun Mao [2,4], Zaixiang Du [2,4], Xiaojun Ke [2,4], Xinjiang Zhang [2] and Yongzhong Zhan [1,2,4,*]

1 School of Materials Science and Engineering, South China University of Technology, Guangzhou 510641, China; ywch053@163.com
2 Guangxi Key Laboratory of Processing for Non-ferrous Metals and Featured Materials, Nanning 530004, China; liumoumiao0524@163.com (M.L.); maojun960621@163.com (J.M.); imzx_to@126.com (Z.D.); kexiaojun@gxu.edu.cn (X.K.); zhangxinjiang1983@163.com (X.Z.)
3 Shenzhen Exit Inspection and Quarantine Bureau Industrial Products Inspection Technology Center, Shenzhen 518067, China; fjlhhp@foxmail.com (J.F.); wujingw@163.com (J.W.)
4 College of Resources, Environment and Materials, Guangxi University, Nanning 530004, China
* Correspondence: zyzmatres@aliyun.com; Tel.: +86-771-3270152

Received: 9 January 2019; Accepted: 24 January 2019; Published: 31 January 2019

Abstract: A complete understanding of the solid-state phase equilibria of the ternary Al–Sn–Y system is essential for the development of both Al-based structural materials and Sn-based lead-free solders. In this work, the phase relationships in the Al–Sn–Y ternary system at 473 K were investigated mainly by means of X-ray powder diffraction (XRD), differential scanning calorimetry (DSC) and scanning electron microscopy (SEM) with energy disperse spectroscopy (EDS) analysis. The existence of 12 binary compounds, namely Sn_3Y, Sn_5Y_2, Sn_2Y, $Sn_{10}Y_{11}$, Sn_4Y_5, Sn_3Y_5, AlY_2, Al_3Y_5, Al_2Y_3, AlY, Al_2Y and α–Al_3Y, was confirmed. Controversial phases (Sn_5Y_2 and Al_3Y_5) were found in this work. This isothermal section consisted of 15 single-phase regions, 27 two-phase regions and 13 three-phase regions. No ternary compounds were found and none of the other phases in this system revealed a remarkable solid solution at 473 K.

Keywords: Al–Sn–Y ternary system; Al_3Y_5 phase; phase equilibrium

1. Introduction

Al–based alloys, which consist of Al–Pb and Al–Sn, are widely used for sliding bearing applications due to their good load carrying capacity, fatigue resistance, wear resistance and sliding properties [1–3]. However, because of toxic Pb, environmental legislation has driven manufacturers to eliminate Pb from bearing alloys. Thus, the focus has been concentrated on Al–Sn alloys. Al–Sn based alloys are simple eutectic binary alloy systems with solid solutions of a wide range of compositions and are well known as soft tribological alloys [3]. However, the main challenges of Al–Sn based alloys are that the strength of alloys is generally low and can easily form a near-continuous large Sn zone that weakens the interface bonding [4]. Abundant attempts, such as alloying addition, to improve preparation methods have been made to overcome those drawbacks. Al–Sn–Si [5], Al–Sn–Bi [6] and Al–Sn–Mg [4] alloys have been researched with the aim of enhancing the strength of Al-based bearing alloys. It is well known that the addition of small amounts of rare earth elements can improve the microstructures and properties of aluminum alloys [7–9]. Meanwhile, Sn–Al eutectic alloy has the potential to be a new system of lead-free solder because it is similar to existing systems, such as the Sn–Zn system and the Sn–Cu system. Rare earth (RE) is an important kind of alloying additive for metallic materials which can significantly improve the properties of alloys by affecting microstructure

and refining grain. The ternary Al–Sn–Y system [10] has been reported before but it is only part of the section (65 at.% Y or less) at room temperature, which is not enough for the application of alloys at high temperatures.

Therefore, a complete knowledge of the phase diagram of the ternary Al–Sn–Y system is essential for a better understanding of this system. The work presented in this article aims to determine the Al–Sn–Y phase equilibrium at 473 K. It is expected that this study will give further insights into the Al–Sn–Y ternary system for practical applications.

2. Materials and Methods

Aluminum (99.9 wt.%), tin (99.9 wt.%) and yttrium (99.99 wt.%) were prepared as raw materials. The alloy compositions of all the samples are plotted in Figure 1. Some components were repeatedly designed for the ideal results. The samples (each 1.5 g) were prepared in an electric arc furnace under an argon atmosphere and a water-cooled copper crucible. In order to obtain a homogeneous composition, each sample was melted three times. For most alloys, the weight loss was generally less than 1 wt.% after being melted. All the samples were sealed in an evacuated quartz tube for homogenization treatment. The alloys which contained more than 50 at.% Sn were homogenized at 673 K for 20 days. Then, the alloys were cooled down to 473 K and maintained for 30 days. Others were kept at 873 K for 10 days and then cooled slowly to 473 K and maintained for 30 days. Finally, all the samples were quenched with ice-water.

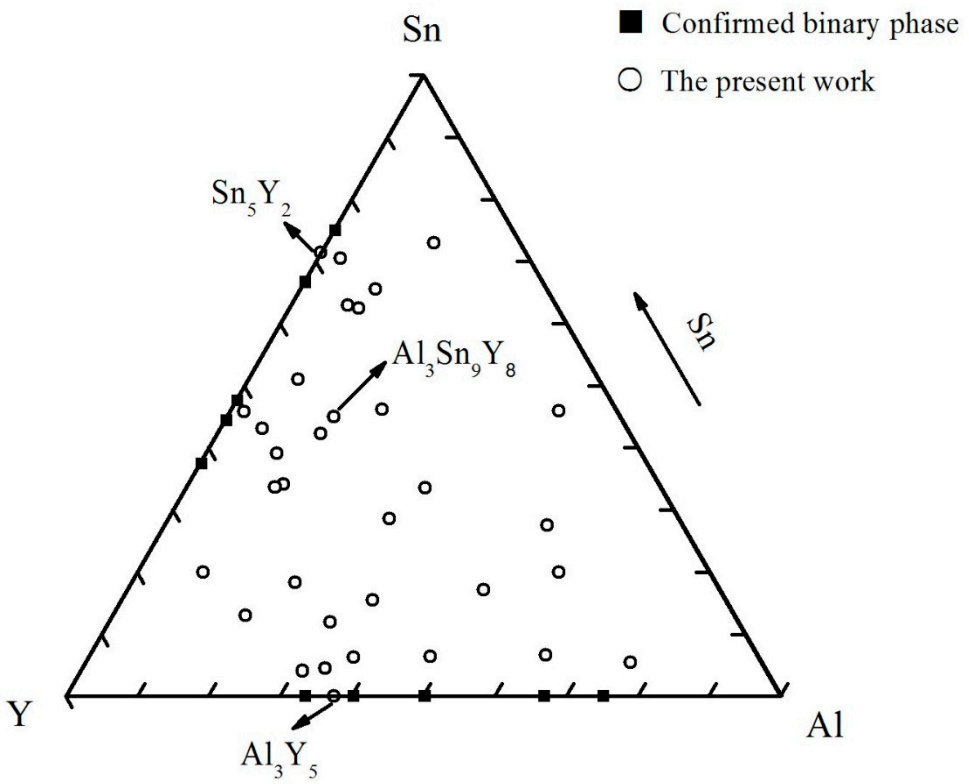

Figure 1. The nominal alloy compositions for the Al–Sn–Y ternary system.

All of the homogenized samples were ground into powder and then measured with the help of a Rigaku D/Max 2500V diffractometer (Rigaku, Tokyo, Japan) with CuKα radiation and a graphite monochromator operated at 40 kV, 200 mA. The microstructures and phase analyses were determined by scanning electron microscopy (SEM, Hitachi, Tokyo, Japan) with energy disperse spectroscopy (EDS, Hitachi, Tokyo, Japan) analysis. The temperature of the phase transition was determined using a differential scanning calorimeter (Netzsch, Bavaria, Germany), which was performed in an aluminum

crucible with a flowing argon atmosphere as a reference substance between room temperature and 1373 K. The heating and cooling rate used was 10 K·min^{-1}.

3. Results

3.1. Sn–Y Binary System

For the Sn–Y binary system, the existence of the five phases, i.e., Sn_3Y, Sn_2Y, $Sn_{10}Y_{11}$, Sn_4Y_5 and Sn_3Y_5, are accepted without question. However, the existence of the phase Sn_5Y_2 is controversial. In the Sn–Y phase diagram revised by Okamoto [11], the phase Sn_5Y_2 was discovered at the range of temperature from 273 K to 798 K and the structure of the Sn_5Y_2 phase was reported in detail, which is in good agreement with the findings of Tang et al. [12]. In that work, the Sn–Y system was investigated by thermodynamic modeling. The Sn_5Y_2 phase was considered to have the same structure as the Ge_5Er_2 phase, and the lattice parameters were 0.4322 nm (a), 0.4409 nm (b) and 1.9089 nm (c). But the existence of the Sn_5Y_2 phase was questioned by Mudryk et al. [13]. When they investigated the R–Fe–Sn ternary systems (R–Y, Gd) at 670 K, Chen et al. [10] and Zhan et al. [14] also reported the same results that phase Sn_5Y_2 was not found. However, Romaka et al. [15] later confirmed the existence of the Sn_5Y_2 phase in the Sn–Ni–Y ternary system at 670 K.

In this work, the samples (60.5 at.% Sn, 12.5 at.% Al, 27 at.% Y, 64.5 at.% Sn, 12.5 at.% Al and 23 at.% Y) were prepared to verify the existence of the Sn_5Y_2 phase. Figure 2 shows the X-ray powder diffraction (XRD) pattern of the sample (60.5 at.% Sn, 12.5 at.% Al and 27 at.% Y), which illustrates the existence of Sn_2Y, Sn_5Y_2 and Al. Figure 3 shows the pattern prepared with the atomic proportion of 64.5 at.% Sn, 12.5 at.% Al and 23 at.% Y. It indicates the existence of the three phases—Sn_3Y, Sn_5Y_2 and Al. In Figures 2 and 3, the Sn phase was found. A possible reason for this is that when the Sn content is higher, it is easy to separate out tin whiskers during annealing over a longer time [16,17]. However, the XRD patterns of the samples clearly showed the existence of the Sn_5Y_2 phase, which was confirmed in the Al–Sn–Y ternary system at this investigated temperature.

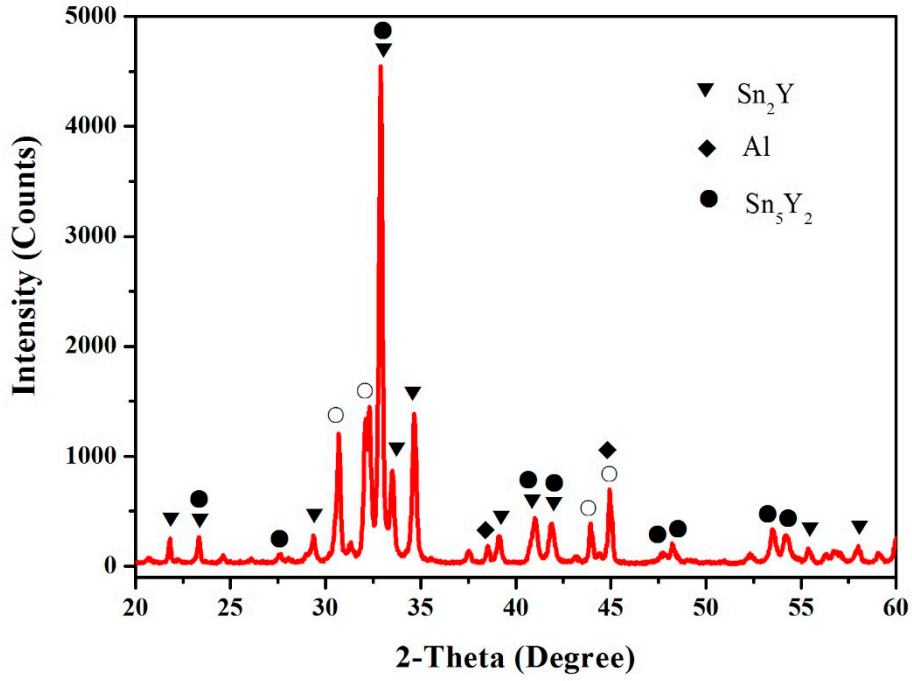

Figure 2. The X-ray powder diffraction (XRD) pattern of the sample (60.5 at.% Sn, 12.5 at.% Al and 27 at.% Y). The symbol ○ is used to indicate Sn.

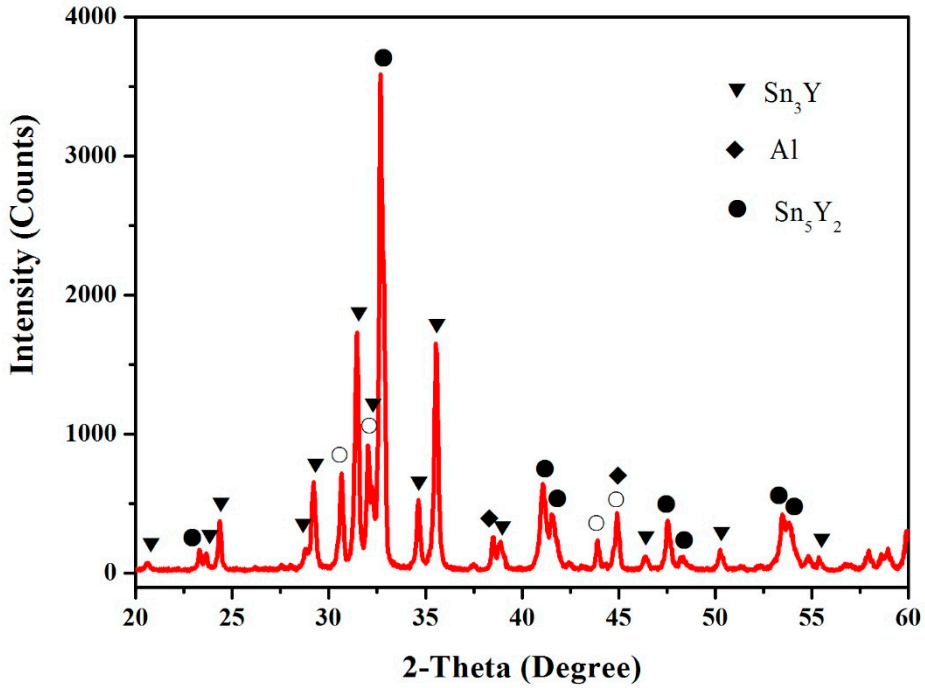

Figure 3. The XRD pattern of the sample (64.5 at.% Sn, 12.5 at.% Al, 23 at.% Y). The symbol ○ is used to indicate Sn.

3.2. Al–Y Binary System

For the Al–Y binary system, the existence of the five phases, i.e., Y_2Al, Y_3Al_2, YAl, YAl_2 and YAl_3, are accepted without question. Bailey [18] reported early on that two structurally related polymorphic forms of Al_3Y have been corroborated—a low temperature form with the hexagonal Ni_3Sn-type structure (α–YAl_3) and a high temperature form with a rhombohedra $BaPb_3$-type structure (β–YAl_3). At the temperature of this work, the YAl_3 phase is α–YAl_3. The Al–Y binary system was also investigated thermodynamically by Lukas [19]. The Y_5Al_3 phase was found by Lukas and the structure of Y_5Al_3 phase was identified by Richter et al. [20]. Liu et al. [21] also experimentally investigated the Al–Y phase diagram and failed to confirm the existence of the Y_5Al_3 phase. After that, in the studies of many ternary systems, such as Al–Fe–Y [22], Al–Zr–Y [23], Al–Sb–Y [24] and Al–Sn–Y [10], the Y_5Al_3 phase was not found. However, Liu et al. [25] thermodynamically assessed the Al–Zn–Y system and found that the binary compound Y_5Al_3 forms through the reaction L + Y_3Al_2 ⇔ Y_5Al_3 + YZnAl at 997 K. However, the temperature range of Y_5Al_3 has not been clearly identified.

In order to obtain a believable result, the samples (4 at.% Sn, 35 at.% Al, 61 at.% Y, 5 at.% Sn, 30 at.% Al and 65 at.% Y) were prepared. Figure 4 shows that the XRD pattern of the sample (4 at.% Sn, 35 at.% Al and 61 at.% Y) illustrates the existence of Y_3Al_2, Y_5Al_3 and Sn_3Y_5. The XRD pattern of the sample (5 at.% Sn, 30 at.% Al, 65 at.% Y) illustrates the existence of Y_2Al, Y_5Al_3 and Sn_3Y_5, as shown in Figure 5, which indicates the existence of the Y_5Al_3 phase.

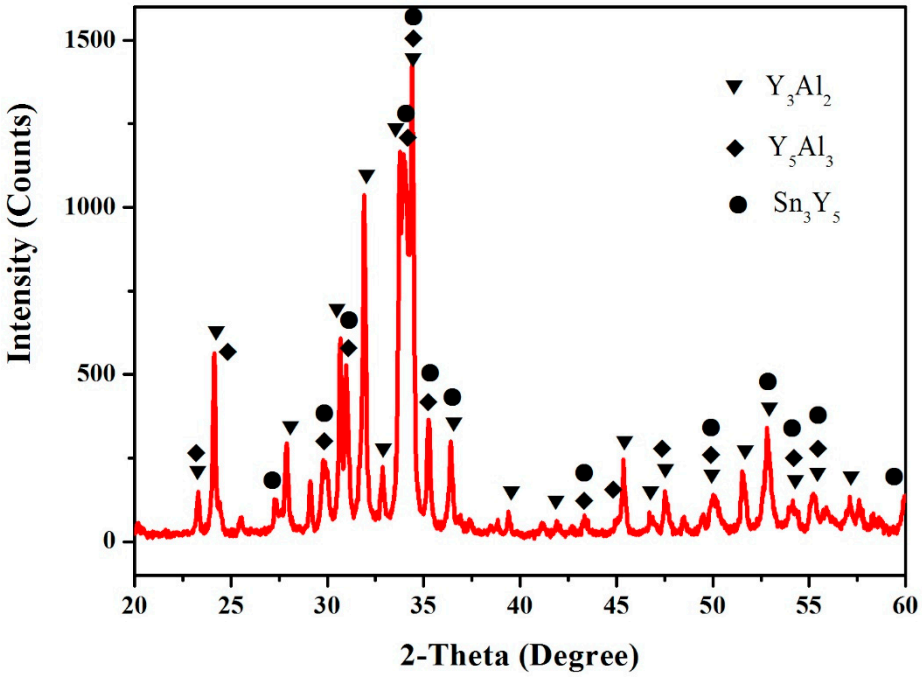

Figure 4. The XRD pattern of the sample (4 at.% Sn, 35 at.% Al and 61 at.% Y).

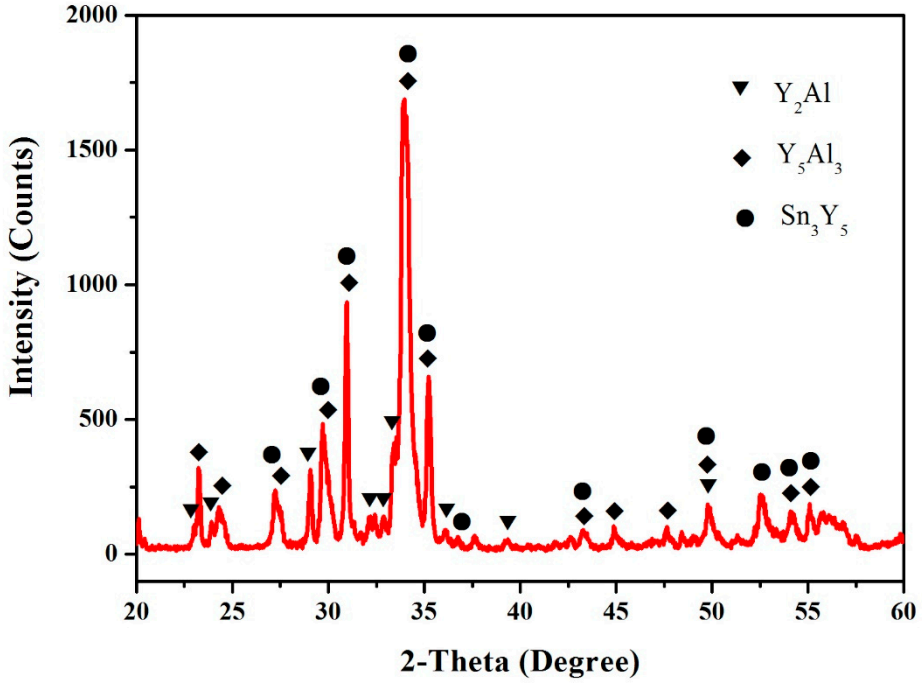

Figure 5. The XRD pattern of the sample (5 at.% Sn, 30 at.% Al, 65 at.% Y).

3.3. Sn–Al Binary System

There was no compound found in the Sn–Al system. Figure 6 shows that the XRD pattern of the sample (69.8 at.% Sn, 14.9 at.% Al, 15.3 at.% Y) illustrates the existence of Sn, Al and Sn_3Y. The crystal structure data of the intermetallic compounds in the Sn–Y, Al–Y and Sn–Al binary systems at 473 K are given in Table 1.

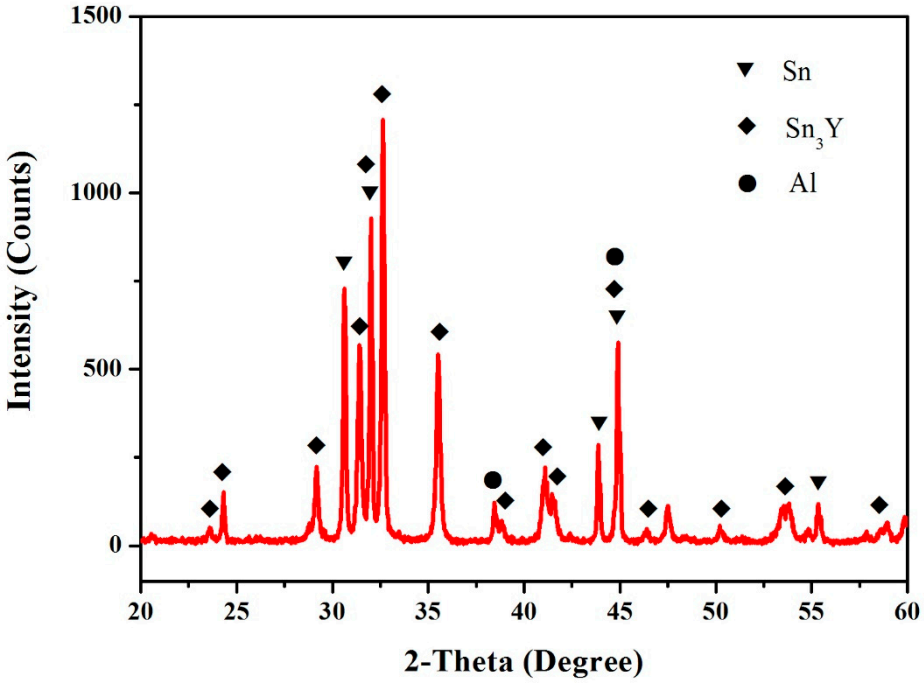

Figure 6. The XRD pattern of the sample (69.8 at.% Sn, 14.9 at.% Al, 15.3 at.% Y).

Table 1. Binary crystal structure data of the Al–Sn–Y system at 473 K.

Phase	Pearson's Symbol	Crystal Structure	Space Group	Lattice Parameters (nm)			Refs.
				a	b	c	
Sn_3Y	oC16	Gd_4Sn_{11}	Amm2	0.4345	0.4391	2.1937	[12]
Sn_5Y_2	oP14	Ge_5Er_2	Pmmm	0.4322	0.4409	1.9089	[12]
Sn_2Y	oC12	Si2Zr	Cmcm	0.4398	1.632	0.4304	[12]
$Sn_{10}Y_{11}$	tI84	$Ge_{10}Ho_{11}$	I4/mmm	1.154	–	1.692	[12]
Sn_4Y_5	oP36	Ge_4Sm_5	Pnma	0.805	1.529	0.805	[12]
Sn_3Y_5	hP16	Si_3Mn_5	$P6_3/mcm$	0.8902	–	0.6536	[12]
αYAl_3	hP8	Ni_3Sn	$P6_3/mmc$	0.6276	–	0.4582	[26]
YAl_2	cF24	Cu_2Mg	$Fd\bar{3}m$	0.78611	–	–	[26]
YAl	oC8	CrB	Cmcm	0.3884	1.1522	0.4385	[26]
Y_3Al_2	tP20	Al_2Zr_3	$P4_2/mnm$	0.8239	–	0.7648	[26]
Y_2Al	oP12	Co_2Si	Pnma	0.6642	0.5084	0.9469	[26]
Y_5Al_3	hP16	Mn_5Si_3	$P6_3/mcm$	0.8787	–	0.6435	[20]

3.4. Al–Sn–Y Ternary System

For the Al–Sn–Y ternary system, the $Al_3Sn_9Y_8$ ternary compound was detected by Chen et al. [10] at room temperature. In order to verify the existence of the $Al_3Sn_9Y_8$ phase at 473 K, the samples (48.5 at.% Sn, 10 at.% Al, 41.5 at.% Y; 41 at.% Sn, 15 at.% Al, 44 at.% Y; 45 at.% Sn, 15 at.% Al, 40 at.% Y) were prepared. The XRD patterns of the samples clearly indicated the existence Sn_2Y, $Sn_{10}Y_{11}$ and YAl_2, as shown in Figure 7. Thus, the $Al_3Sn_9Y_8$ ternary compound was not detected in this work.

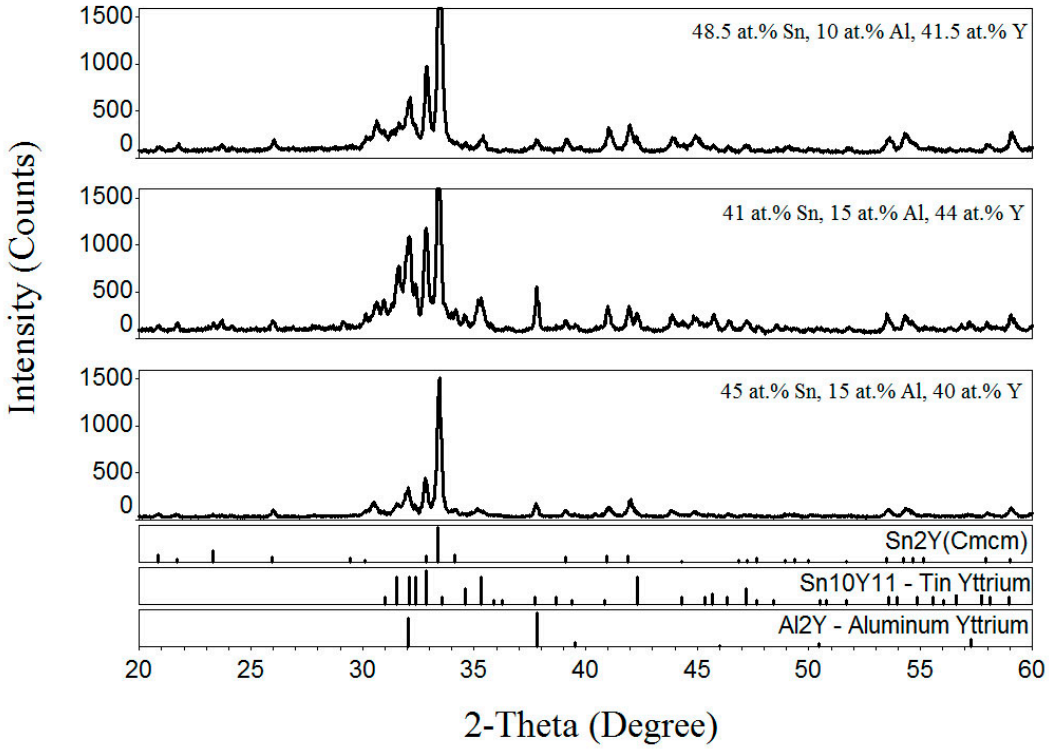

Figure 7. The XRD patterns of the samples (48.5 at.% Sn, 10 at.% Al, 41.5 at.% Y, 41 at.% Sn, 15 at.% Al, 44 at.% Y and 45 at.% Sn, 15 at.% Al, 40 at.% Y).

3.5. Isothermal Section

According to the XRD, SEM/EDS and differential scanning calorimeter (DSC) analysis, the isothermal section of the Al–Sn–Y ternary system at 473 K is shown in Figure 8. This isothermal section consists of 15 single phase regions, 27 binary phase regions and 13 ternary phase regions. No ternary compounds were found and none of the other phases in this system revealed a remarkable homogeneity range at 473 K. Figure 9 shows the XRD pattern of the sample (20 at.% Sn, 9 at.% Al, 71 at.% Y) indicating the existence of Sn_3Y_5, Y_2Al and Y. The XRD pattern of the equilibrated sample with a stoichiometric composition of 6.5 at.% Sn, 47.8 at.% Al, 45.7 at.% Y indicated the existence of Sn_3Y_5, Al_2Y and YAl, as shown in Figure 10. In addition, Figure 11 shows the XRD pattern of the sample (39 at.% Sn, 10 at.% Al, 51 at.% Y) indicating the existence of Sn_4Y_5, Al_2Y and $Sn_{10}Y_{11}$. Figure 12 shows the XRD pattern of the sample (6.5 at.% Sn, 64 at.% Al, 29.5 at.% Y) indicating the existence of α–Al_3Y, Al_2Y and Sn_2Y. The XRD results confirm that nine binary compounds, namely Sn_3Y, Sn_2Y, $Sn_{10}Y_{11}$, Sn_4Y_5, Sn_3Y_5, Y_2Al, Y_3Al_2, YAl, YAl_2 and α–YAl_3, exist in this system at 473 K. The SEM photographs (as shown in Figures 11–15) also clearly display the existence of some phases (identified by EDS). Constitutions of the ternary phase regions and compositions of the typical alloys are given in Table 2.

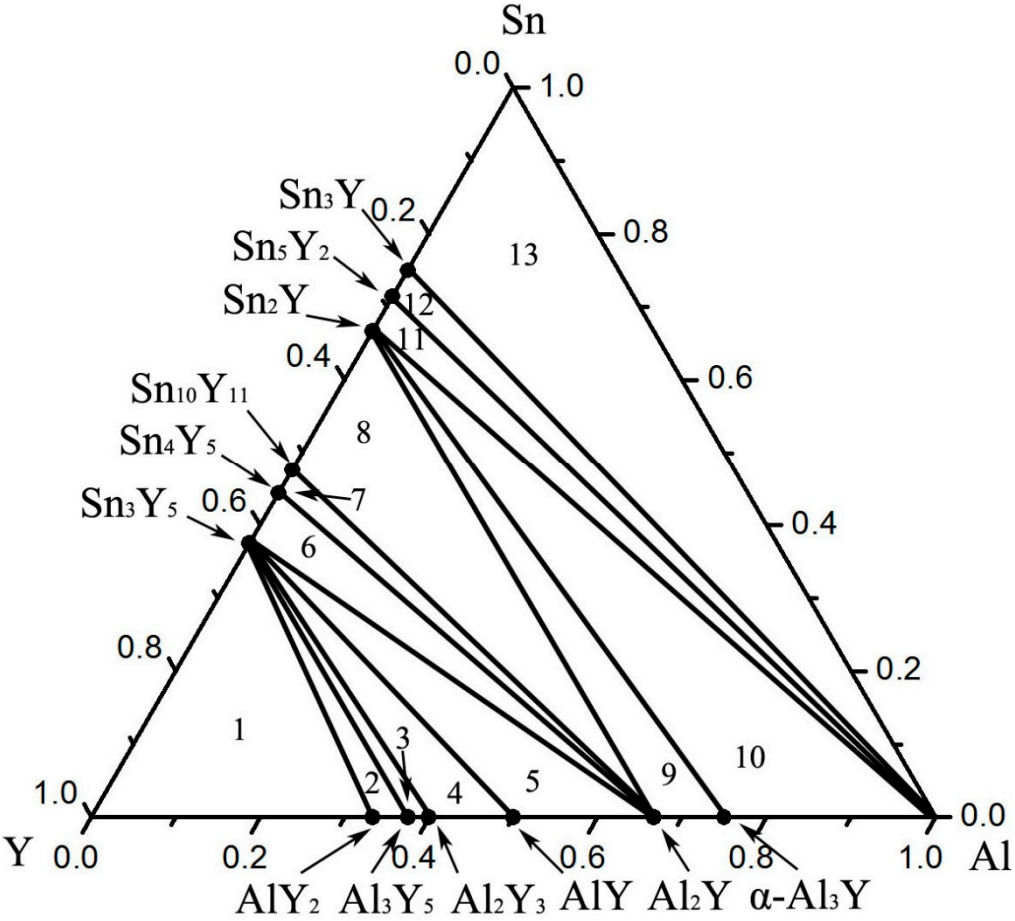

Figure 8. The isothermal section of the Sn–Al–Y ternary system at 473 K.

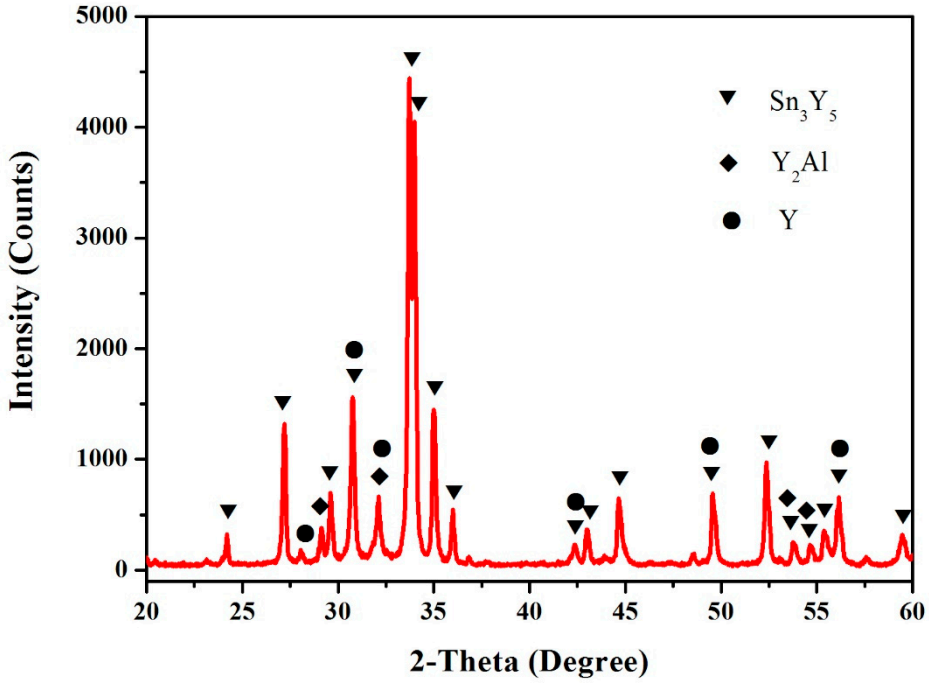

Figure 9. The XRD pattern of the sample (20 at.% Sn, 9 at.% Al and 71 at.% Y).

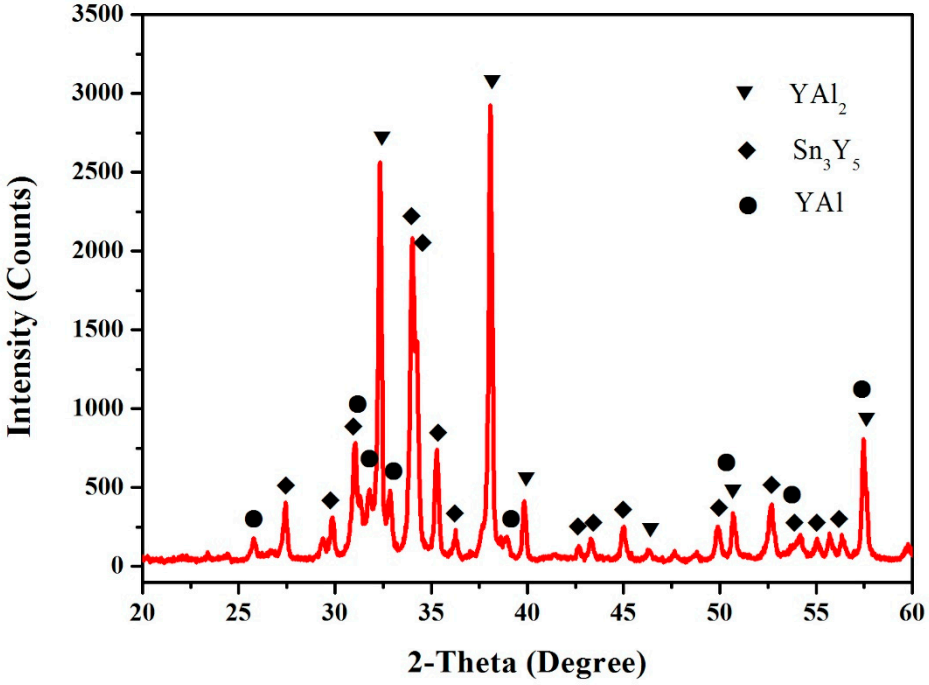

Figure 10. The XRD pattern of the sample (6.5 at.% Sn, 47.8 at.% Al and 45.7 at.% Y).

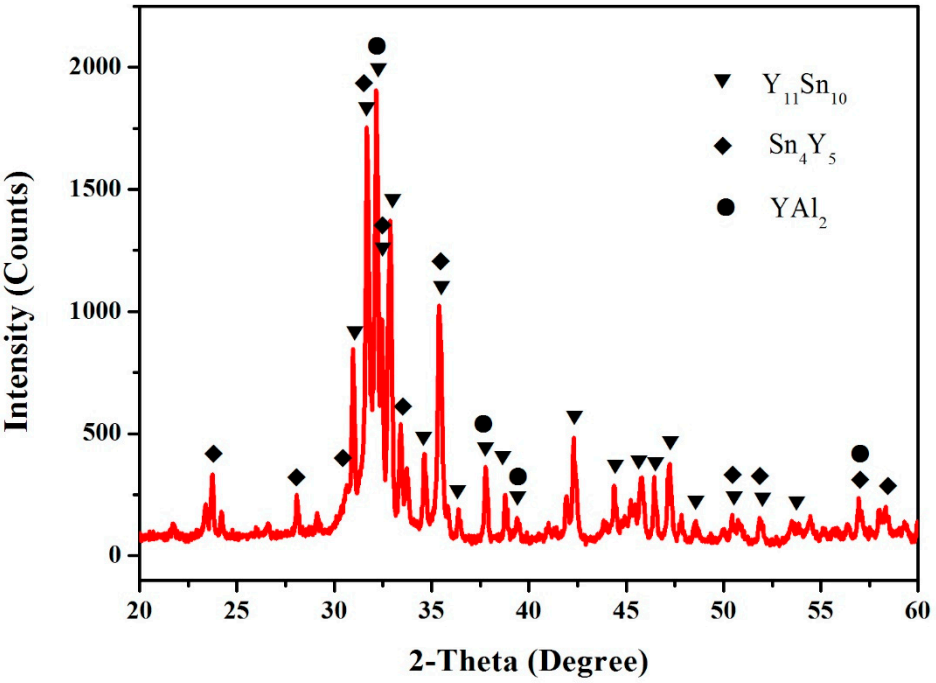

Figure 11. The XRD pattern of the sample (39 at.% Sn, 10 at.% Al and 51 at.% Y).

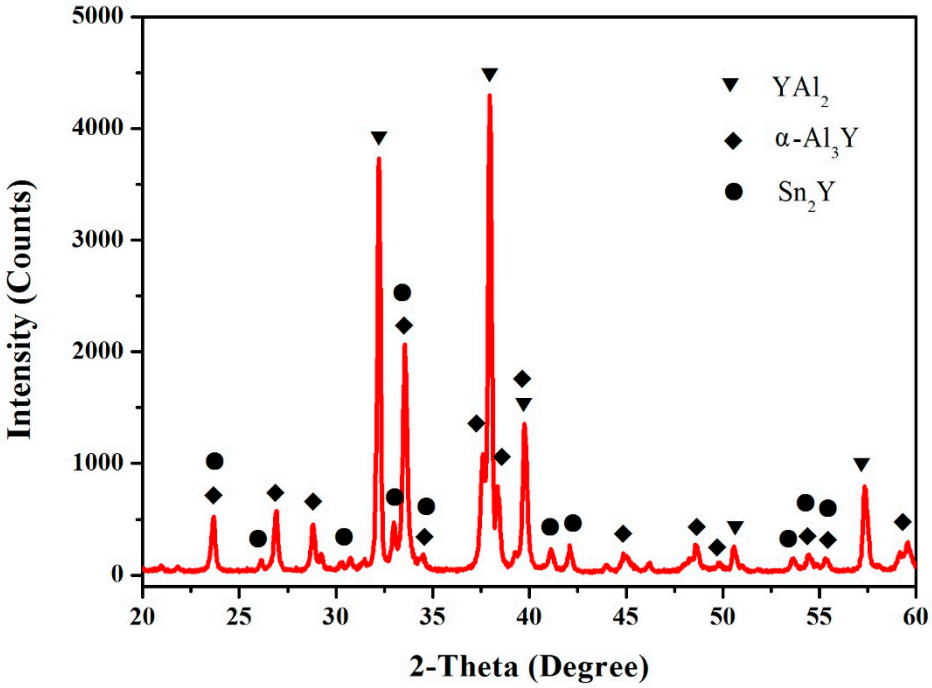

Figure 12. The XRD pattern of the sample (6.5 at.% Sn, 64 at.% Al and 29.5 at.% Y).

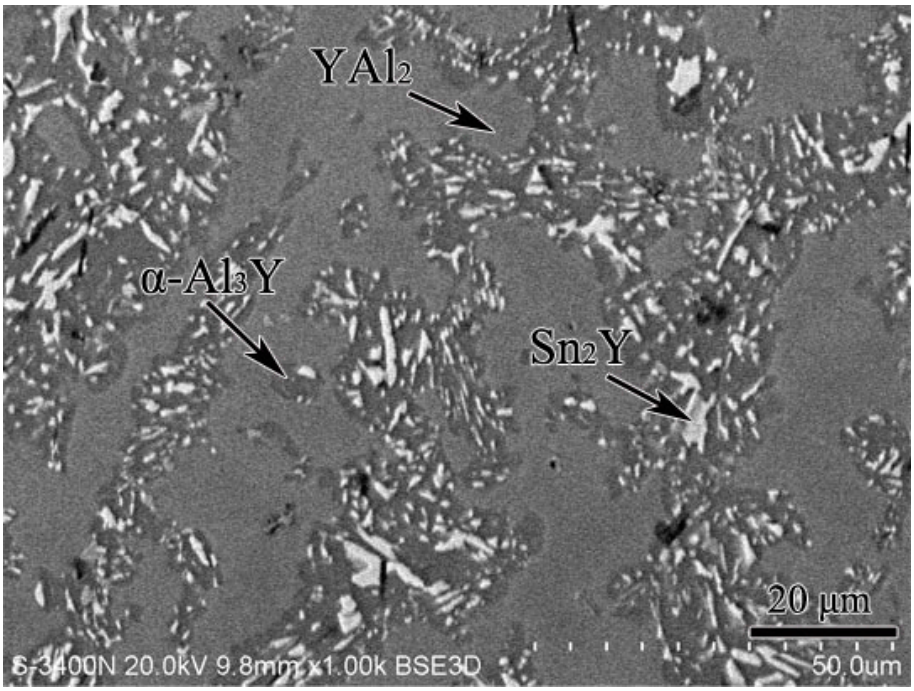

Figure 13. The scanning electron microscopy (SEM) micrograph of the equilibrated alloy 6.5 at.% Sn, 64 at.% Al, 29.5 at.% Y illustrating the existence of YAl_2, Sn_2Y and α–Al_3Y.

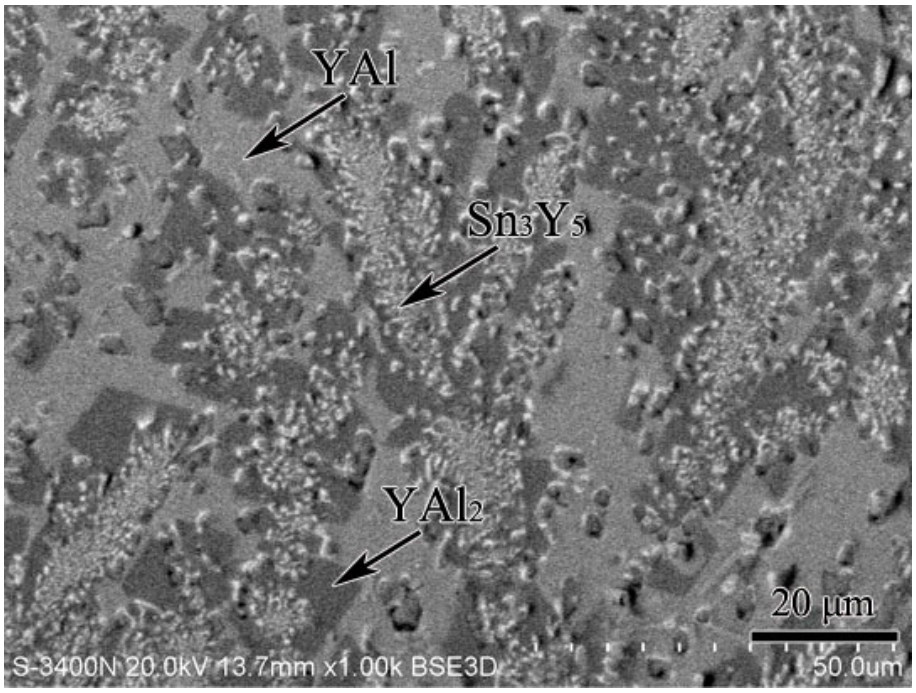

Figure 14. The SEM micrograph of the equilibrated alloy 6.5 at.% Sn, 47.8 at.% Al, 45.7 at.% Y illustrating the existence of YAl, YAl_2 and Sn_3Y_5.

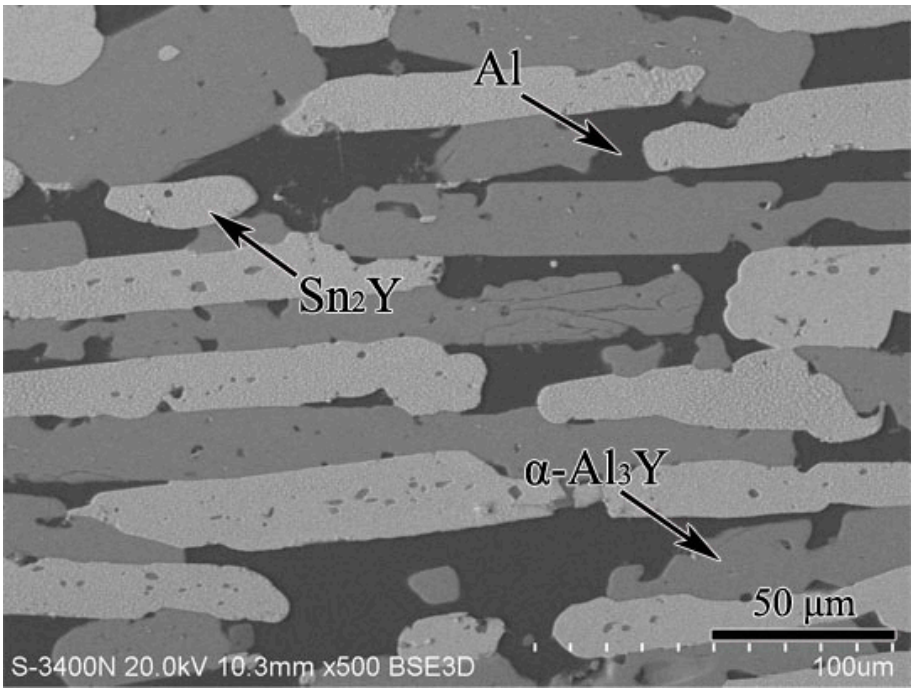

Figure 15. The SEM micrograph of the equilibrated alloy 20 at.% Sn, 59 at.% Al, 21 at.% Y illustrating the existence of Al, Sn_2Y and α–Al_3Y.

Table 2. Details of the phase regions and typical samples in the Al–Sn–Y system at 473 K.

Phase Regions	Alloy Composition (at.%)			Phase Composition
	Sn	Al	Y	
1	20	9	71	$Y + Sn_3Y_5 + Y_2Al$
2	5	30	65	$Y_2Al + Sn_3Y_5 + Y_5Al_3$
3	4	35	61	$Y_5Al_3 + Sn_3Y_5 + Y_3Al_2$
4	6.3	37	56.7	$Y_3Al_2 + Sn_3Y_5 + AlY$
5	6.5	47.8	45.7	$AlY + Sn_3Y_5 + Al_2Y$
6	33.5	12.5	54	$Al_2Y + Sn_3Y_5 + Sn_4Y_5$
7	39	10	51	$Sn_4Y_5 + Al_2Y + Sn_{10}Y_{11}$
8	45	15	40	$Sn_{10}Y_{11} + Al_2Y + Sn_2Y$
9	6.5	64	29.5	$Sn_2Y + Al_2Y + \alpha–Al_3Y$
10	20	59	21	$\alpha–Al_3Y + Sn_2Y + Al$
11	60.5	12.5	27	$Al + Sn_2Y + Sn_5Y_2$
12	64.5	12.5	23	$Sn_5Y_2 + Al + Sn_3Y$
13	69.8	14.9	15.3	$Sn_3Y + Al + Sn$

4. Conclusions

The isothermal section of the Sn–Al–Y ternary system at 473 K was experimentally constructed in this work. This isothermal section consists of 15 single-phase regions, 27 two-phase regions and 13 three-phase regions. The existence of 12 binary compounds was confirmed; namely, Sn_3Y, Sn_5Y_2, Sn_2Y, $Sn_{10}Y_{11}$, Sn_4Y_5, Sn_3Y_5, AlY_2, Al_3Y_5, Al_2Y_3, AlY, Al_2Y and $\alpha–Al_3Y$. No ternary compound was found.

Author Contributions: Conceptualization, W.Y. and Y.Z.; Methodology, W.Y. and M.L.; Software, M.L.; Validation, Z.D., J.M. and X.Z.; Formal Analysis, W.Y. and M.L.; Investigation, W.Y. and M.L.; Resources, J.M. and X.Z.; Data Curation, W.Y. and M.L.; Writing-Original Draft Preparation, M.L.; Writing-Review & Editing, W.Y.; Visualization, Y.Z.; Supervision, M.L.; Project Administration, Y.Z.; Funding Acquisition, X.K., J.F. and J.W.

Funding: This research was funded by by [the National Key R&D Program of China] grant number [2016YFB0301400], [the National Natural Science Foundation of China] grant number [51761002, 51668007], [the Training Plan of High-Level Talents of Guangxi University (2015)] and [the science and technology plan projects of Shenzhen Entry-Exit Inspection and Quarantine Bureau] grant number [SZ2017001].

Conflicts of Interest: The authors declare no conflict of interest.

References

1. Liu, X.; Zeng, M.Q.; Ma, Y.; Zhu, M. Wear behavior of Al–Sn alloys with different distribution of Sn dispersoids manipulated by mechanical alloying and sintering. *Wear* **2008**, *265*, 1857–1863. [CrossRef]
2. Ning, X.J.; Jang, J.H.; Kim, H.J.; Li, C.J.; Lee, C. Cold spraying of Al–Sn binary alloy: Coating characteristics and particle bonding features. *Surf. Coat. Technol.* **2008**, *202*, 1681–1687. [CrossRef]
3. Ueda, M.; Inaba, R.; Ohtsuka, T. Composition and structure of Al–Sn alloys formed by constant potential electrolysis in an $AlCl_3$–NaCl–KCl–$SnCl_2$ molten salt. *Electrochim. Acta* **2013**, *100*, 281–284. [CrossRef]
4. Lu, Z.C.; Gao, Y.; Zeng, M.Q.; Zhu, M. Improving wear performance of dual-scale Al–Sn alloys: The role of Mg addition in enhancing Sn distribution and tribolayer stability. *Wear* **2014**, *309*, 216–225. [CrossRef]
5. Kong, C.J.; Brown, P.D.; Harris, S.J.; McCartney, D.G. The microstructures of a thermally sprayed and heat treated Al–20 wt.%Sn–3 wt.%Si alloy. *Mater. Sci. Eng. A* **2005**, *403*, 205–214. [CrossRef]
6. Hou, D.; Li, D.; Han, L.; Ji, L. Effect of lanthanum addition on microstructure and corrosion behavior of Al-Sn-Bi anodes. *J. Rare Earths* **2011**, *29*, 129–132. [CrossRef]
7. Mao, Z.G.; Seidman, D.N.; Wolverton, C. First-principles phase stability, magnetic properties and solubility in aluminum–rare-earth (Al–RE) alloys and compounds. *Acta Mater.* **2011**, *59*, 3659–3666. [CrossRef]
8. Pan, H.; Pan, F.; Yang, R.; Peng, J.; Zhao, C.; She, J.; Gao, Z.; Tang, A. Thermal and electrical conductivity of binary magnesium alloys. *J. Mater. Sci.* **2014**, *49*, 3107–3124. [CrossRef]
9. Zuo, X.R.; Jing, Y.W. Investigation of the age hardening behaviour of 6063 aluminium alloys refined with Ti, RE and B. *J. Mater. Process. Technol.* **2009**, *209*, 360–366. [CrossRef]

10. Chen, R.Z.; Wei, X.Z.; Liu, J.Q. The isothermal section of the phase diagram of the ternary system Al-Sn-Y at room temperature. *J. Alloy. Compd.* **1995**, *218*, 221–223.
11. Okamoto, H. Comment on Sn-Y (Tin-Yttrium). *J. Phase Equilibria* **1995**, *16*, 104. [CrossRef]
12. Tang, C.; Hu, B.; Du, Y.; Zhao, D.; Zhou, P.; Zheng, F.; Gao, Q.; Wang, J. Thermodynamic modeling of the Hf–Sn and Sn–Y systems. *Calphad* **2012**, *39*, 91–96. [CrossRef]
13. Mudryk, Y.; Romaka, L.; Stadnyk, Y.; Bodak, O.; Fruchart, D. X-ray investigation of the R–Fe–Sn ternary systems (R–Y, Gd). *J. Alloy. Compd.* **2004**, *383*, 162–165. [CrossRef]
14. Zhan, Y.; He, L.; Ma, J.; Sun, Z.; Zhang, G.; Zhuang, Y. Experimental study of Ti–Sn–Y system phase equilibria at 473 K. *J. Alloy. Compd.* **2009**, *470*, 173–175. [CrossRef]
15. Romaka, L.; Dovgalyuk, Y.; Romaka, V.V.; Lototska, I.; Stadnyk, Y. Interaction of the components in Y–Ni–Sn ternary system at 770 K and 670 K. *Intermetallics* **2012**, *29*, 116–122. [CrossRef]
16. Hao, H.; Dong, W.X.; Shi, Y.W. Mechanism of Tin Whisker Morphology. *Chin. J. Nonferrous Met.* **2009**, *2*, 021.
17. Hao, H.; Shi, Y.W. Tin whisker growth accelerated by the oxidization of RE-phase on lead-free solder surface. *Electron. Compon. Mater.* **2009**, *8*, 011.
18. Bailey, D.M. The Structures of Two Polymorphic Froms of YAl_3. *Acta Crystallogr.* **1967**, *23*, 729–733. [CrossRef]
19. Lukas, H.L. System Al-Y, Cost 507. *Thermochem. Database Light Met. Alloy.* **1998**, 99–102.
20. Richter, R.; Altounian, Z.; Strom-Olsen, J.O.; Köster, U.; Blank-Bewersdorff, M. Y_5Al_3: A new Y-Al compound. *J. Mater. Sci.* **1987**, *22*, 2983–2986. [CrossRef]
21. Liu, S.; Du, Y.; Xu, H.; He, C.; Schuster, J.C. Experimental investigation of the Al–Y phase diagram. *J. Alloy. Compd.* **2006**, *414*, 60–65. [CrossRef]
22. Feng, H.; Zhang, M.; Chen, H.; Liang, J.; Tao, X.; Ouyang, Y.; Du, Y. Experimental Investigation on Phase Equilibria of Al-Fe-Y System at 773 K. *J. Phase Equilibria Diffus.* **2014**, *35*, 256–261. [CrossRef]
23. She, J.; Zhan, Y.; Hu, Z.; Li, C.; Hu, J.; Du, Y.; Xu, H. Experimental study of Al–Zr–Y system phase equilibria at 773 K. *J. Alloy. Compd.* **2010**, *497*, 118–120. [CrossRef]
24. Zeng, L.M.; Wang, S.Y. The 800 K isothermal section of the Y–Al–Sb phase diagram. *J. Alloy. Compd.* **2003**, *351*, 176–179. [CrossRef]
25. Liu, X.J.; Wen, M.Z.; Wang, C.P.; Pan, F.S. Thermodynamic assessment of the Zn–Y and Al–Zn–Y systems. *J. Alloy. Compd.* **2008**, *452*, 283–290. [CrossRef]
26. Gschneidner, K.A.; Calderwood, F.W. The Al-Y (Aluminum-Yttrium) System. *Bull. Alloy Phase Digrams* **1989**, *10*, 44–47. [CrossRef]